J Mater Sci: Mater Med (2008) 19:3545–3553
DOI 10.1007/s10856-008-3526-y

Silk fibroin/chitosan scaffold: preparation, characterization, and culture with HepG2 cell

Zhending She · Chenrui Jin · Zhi Huang · Bofeng Zhang · Qingling Feng · Yingxin Xu

Received: 15 November 2007 / Accepted: 25 June 2008 / Published online: 15 July 2008

Abstract Tissue engineering requires the development of three-dimensional water-stable scaffolds. In this study, silk fibroin/chitosan (SFCS) scaffold was successfully prepared by freeze-drying method. The scaffold is water-stable, only swelling to a limited extent depending on its composition. Fourier Transform Infrared (FTIR) spectra and X-Ray diffraction curves confirmed the different structure of SFCS scaffolds from both chitosan and silk fibroin. The homogeneous porous structure, together with nano-scale compatibility of the two naturally derived polymers, gives rise to the controllable mechanical properties of SFCS scaffolds. By varying the composition, both the compressive modulus and compressive strength of SFCS scaffolds can be controlled. The porosity of SFCS scaffolds is above 95% when the total concentration of silk fibroin and chitosan is below 6 wt%. The pore sizes of the SFCS scaffolds range from 100 μm to 150 μm, which can be regulated by changing the total concentration. MTT assay showed that SFCS scaffolds can promote the proliferation of HepG2 cells (human hepatoma cell line) significantly. All these results make SFCS scaffold a suitable candidate for tissue engineering.

Z. She · C. Jin · Z. Huang · Q. Feng (✉)
Key Laboratory of Advanced Materials, Department of Materials Science and Engineering, Tsinghua University, Beijing 100084, China
e-mail: biomater@mail.tsinghua.edu.cn

B. Zhang · Y. Xu
Institute of Surgical Research, Chinese PLA General Hospital, Beijing 100853, China

1 Introduction

Severe organ donor shortage, high cost, and life-long requirement of immunosuppressive drugs limit the therapeutic approach of orthotopic liver transplantations, which have saved many patients' lives [1]. Liver tissue engineering, aiming to construct an implantable liver, has the potential to alleviate the organ donor shortage. As an important part of tissue engineering, three-dimensional scaffolds are beneficial, because they provide a place for attachment, increase surface area, support a large cell mass, and are capable of shaping specific structures [2–4]. In order to construct actively metabolizing tissue, liver tissue engineering requires the scaffold to provide the seeded cells with proper environmental cues, factors for growth and either a prevascularized site or a porous structure allowing for angiogenesis [5, 6]. Many synthetic polymers, including polylactic acid (PLA), polyglycolic acid (PGA), and polylactic glycolic acid (PLGA), have been used as three-dimensional scaffold materials [3, 7, 8]. Lack of active groups, slow degradation under physiological condition, and the use of organic solvent which prohibit the addition of cell growth factors, limit the use of synthetic polymers [6, 8, 9]. Various natural polymers such as alginic acid, chitosan (CS), collagen, and silk fibroin (SF) have recently been used as scaffold materials for liver tissue engineering owing to their good biocompatibility. However, they cannot be easily processed into three-dimensional scaffolds with satisfactory stability and mechanical properties [10–13].

SF is an attractive natural fibrous protein for biomedical application due to its permeability to oxygen and water, good cell adhesion and growth characteristics, relatively low thrombogenicity, low inflammatory response, protease susceptibility, and high tensile strength [14, 15]. Removal of the sericin coating before use removes the thrombogenic and

inflammatory responses of SF [16]. SF can exist in two general conformations: random coil and β-sheet form [17]. The conformation transition of SF from a random coil to a β-sheet structure can be induced by some treatments such as heating, stretching, or immersion in polar solvents. This transition makes SF attractive as a biomaterial because SF with a β-sheet structure is resistant to water, while random coil is not [18]. However, pure SF scaffold is very brittle. The physical properties of SF scaffold can be enhanced by mixing it with other synthetic or natural polymers, such as poly-(vinyl alcohol) (PVA), collagen, CS, and so forth [13, 19, 20].

CS is a partially deacetylated product of chitin, a crystalline polysaccharide found in crustaceans and insects, which is structurally similar to glycosaminoglycans [21]. The good potential of CS as a biomaterial derives from its cationic and high-charge density properties, which allow CS to form insoluble ionic complexes with a variety of anionic polymers. CS has also been shown to have wound healing properties, to be nontoxic, and to have minimal foreign body response with accelerated angiogenesis [22]. In addition, the free amino groups of CS can be chemically derivatized in mild reaction conditions to promote biological activities and modify mechanical properties [20, 23–27]. One disadvantage of using CS alone as a scaffold is that it is difficult to control its degradation and swelling properties in aqueous solution. So combining CS with other polymers is a good choice to get suitable scaffolds.

Gobin et al. [13] acquired three-dimensional scaffold by blending SF and CS. After treatment with methanol and sodium hydroxide, the scaffolds shrank significantly, so it is not water-stable. Aiming to get three-dimensional porous water-stable SFCS scaffold, we employed another experimental path to mix SF with CS.

In this study, we prepared the blend of SF and CS as a water-stable scaffold. The morphology, structure and mechanical properties, as well as the HepG2 cell culture behavior of the SFCS scaffolds, were investigated.

2 Materials and methods

2.1 Materials

Bombyx mori silkworm silk was purchased from Yi Xian Raw Silk Factory in China. Chitosan (80% deacetylated, molecular weight: 5.3×10^4) and PLA (molecular weight: 1.0×10^5) was purchased from Shandong Medical Appliance Factory in China.

2.2 Preparation of silk fibroin aqueous solution

The sericin coating on raw silk was removed via degumming. In brief, 0.5% (w/v) sodium carbonate was dissolved and brought to 100°C. Raw silk was added at 1.875:100 w/v and heated for 1 h. The alkaline soap solution was then drained and the degummed silk was rinsed by tap water for 20 times. Finally, any remaining sericin was removed completely by rinsing the silk in running deionized water. The washed silk was then air-dried.

A calcium dichloride-ethanol solution was prepared, with molar ratio $CaCl_2$:H_2O:C_2H_5OH 1:8:2.5. The silk fibroin was dissolved in the solution above with 12% (w/v) concentration at 80°C for one hour by continuous stirring. The solution was cooled and then dialyzed against deionized water for 3 days. After vacuum filtration, the silk fibroin aqueous solution was stored at 4°C until use. The concentration of silk fibroin aqueous solution was determined by weighing the remaining solid after drying. The final silk fibroin concentration can be adjusted to meet the need by concentrating the solution at 60°C or diluting [11, 28].

2.3 Fabrication of SFCS scaffolds

Chitosan solution was prepared by dissolving 3 wt% chitosan in 1.2 wt% acetic acid. An equal volume of the same concentration of silk fibroin was added to prepare a 1.5 wt%–1.5 wt% blend and the solution was allowed to mix for 15 min. The blended solution was then poured into polytetrafluoroethene columniform molds (diameter, 10 mm; height, 25 mm), frozen overnight in a −20°C freezer, followed by lyophilization for 48 hours. The dry samples were removed from the molds and treated in methanol for 2 hours. Finally, after another 48 hours of lyophilization, the SFCS scaffolds were prepared. Scaffolds with different composition can be acquired by changing either the concentration or the volume proportion of silk fibroin solution and chitosan acetic acid solution before blending.

2.4 Scanning electron microscopy (SEM)

SFCS scaffolds were fractured in liquid nitrogen using a razor blade. Samples were sputter coated with gold. The morphology of the scaffolds was observed with a LEO Gemini 1530 Field Emission Gun SEM.

2.5 X-ray diffraction

A Rigaku D/max X-ray diffractometer (CuKα; 40 kV; 120 mA; λ, 1.5405 Å; rate, 4 deg min^{-1}) was used for the study.

2.6 FTIR spectroscopy

Approximately 1 mg of freeze-dried samples were pressed into a pellet with 200 mg of potassium bromide and FTIR spectra were recorded with an accumulation of 256 scans

and a resolution of 4 cm^{-1} on a Nicolet 560 system (America).

2.7 Mechanical properties

Resistance to mechanical compression of the scaffolds was performed on an Instron-6022 equipped with a 0.1 kN load cell at room temperature. The crosshead speed was set at 0.5 mm min^{-1}. Three samples were evaluated for each composition. Cylinder-shaped samples measuring 9 mm in diameter and 12 mm in height were used. The compressive stress and strain were graphed and the average compressive strength as well as the compressive modulus and standard deviation were determined. The compressive modulus was defined by the slope of the initial linear section of the stress–strain curve. The compressive strength was determined by drawing a line parallel starting at 1% strain. The point at which this line crossed the stress–strain curve was defined as the compressive strength of the scaffold [29].

2.8 Porosity

The porosity of the scaffolds was measured by mercury intrusion porosimetry (Atopore III 9510, Micromeritics, America). To determine the porosities, it was assumed that the shape of the pores is cylinder. The contact angle of mercury is 130°, and the surface tension of mercury is 0.485 N m^{-1}.

2.9 HepG2 cell culture

MTT assay is a quantitative colorimetric assay for mammalian cell survival and cell proliferation [30]. It is an indirect method for assessing cell growth and proliferation, since mitochondria oxidize the thiazolyl blue (MTT) solution, giving a typical blue–violet end-product, O.D. value of 490 nm can be quantified to cell number.

HepG2 cells (supplied by the Chinese Academy of Military Medical Sciences) were cultured in DMEM medium supplemented with 10% fetal bovine serum, 200 mM L-glutamine, 2 mg ml^{-1} sodium bicarbonate and 100 mg ml^{-1} penicillin/streptomycin. The cells were cultured in 37.5 cm^2 flasks at 37°C in a humidified atmosphere of 5% CO_2. Confluent monolayers were split by treatment with sterile phosphate-buffered saline (PBS) and 0.05% trypsin/EDTA solution, and the culture medium was replaced every 3 days. Samples were cut into circular discs suitably sized for 24-well tissue culture plate wells. The circular matrices were sterilized with 70% alcohol under ultraviolet light overnight and then rinsed extensively three times with sterile PBS. Before cell culturing, scaffolds were pre-wetted by immersion in DMEM for 12 h in the 37°C incubator.

HepG2 cells were cultured onto PLA and SFCS scaffolds ($n = 4$; diameter, 9 mm; hight, 1 mm) for 3 and 5 days at 37°C under an atmosphere of 5 % CO_2 and 95 % air, with the original cell culture density of 4,000 cells $well^{-1}$. Then the culture medium was replaced with serum free culture medium containing MTT (0.5 mg ml^{-1}). Cultured for 4 h, the samples were transferred to 2 ml plastic tubes. Tubes were centrifuged for 5 min at 8,000 rpm, and then the supernatant was aspirated. After DMSO was added into each tube, samples were cut into pieces and disintegrated using a Microbeater. Tubes were centrifuged at 8,000 rpm for 10 min. The solution of each sample was aspirated into a microtiter plate and the absorbance at 490 nm was measured on a SS-300 Immunoanalyzer.

2.10 Statistical analysis

Differences between data sets were analyzed by analysis of variance (ANOVA) and multiple t tests. $P \leq 0.05$ was considered statistically significant.

3 Results

3.1 Morphology and water-stable property

Before treatment with methanol, SFCS scaffolds dissolved rapidly in water. However, methanol-treated SFCS scaffolds are water-stable. They just swelled to a limited extent according to the SFCS composition.

Figure 1 shows the SEM images of SFCS scaffolds with a series of total concentration or SF concentration. Extremely high concentration of SF (8.76 wt%, Fig. 1a) results in sheet-like structure, with small pores (about 20 μm in diameter) interconnected between sheets. When the total concentration is below 6 wt%, all SFCS scaffolds show homogeneous porous structure. Keeping CS concentration at a constant 2 wt%, with the decrease of SF concentration, pore sizes increase, in a range from 100 μm to 150 μm (Fig. 1b–d). When the total concentration is kept at 3 wt% (Fig. 1d–e), or 4 wt% (Fig. 1c, f), the changes of SF content has only little effect on the morphology of the porous structure and pore size.

Figure 2 shows SEM images of the pore wall surface and section morphology of SFCS scaffold with 1 wt% SF-2 wt% CS. The pore wall has a smooth surface morphology. The width of the pore wall is about 1 μm.

3.2 Structural analysis

To confirm the conformational changes, X-ray diffraction curves of SFCS scaffolds were examined (Fig. 3). Pure

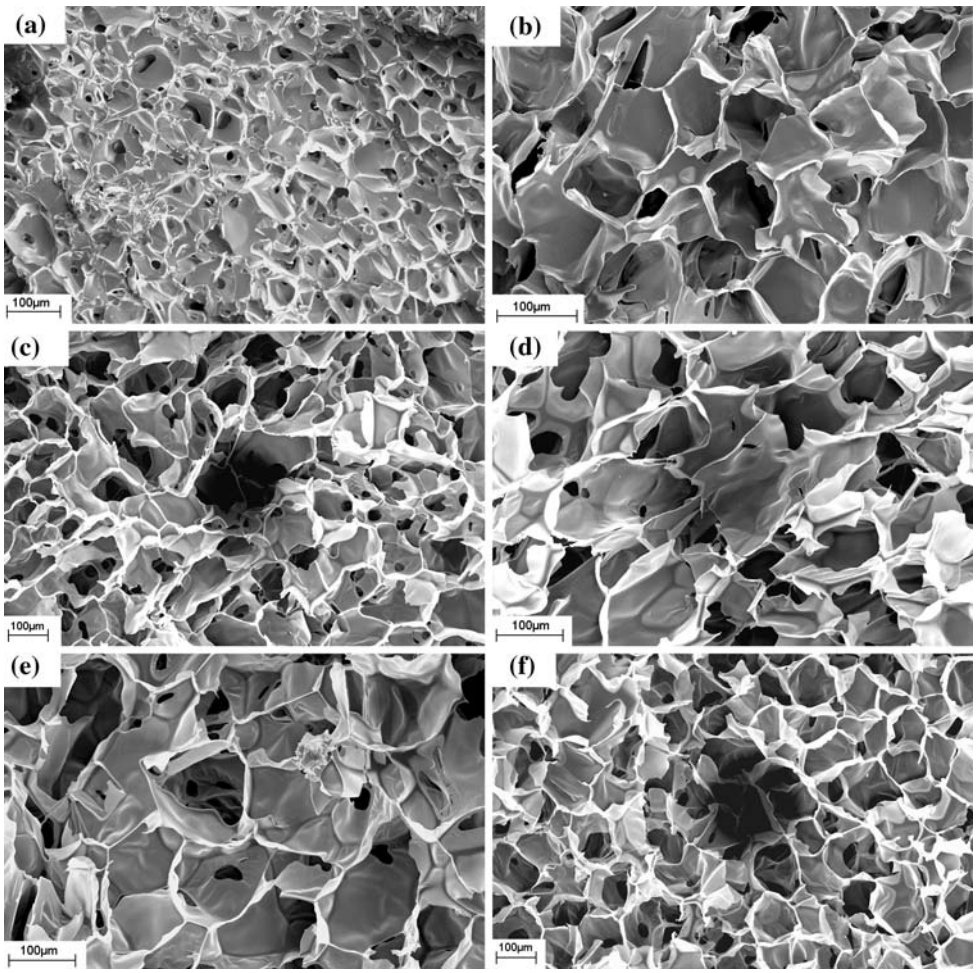

Fig. 1 SEM images of porous SFCS scaffolds prepared from silk fibroin-chitosan aqueous solutions. The pore size increases with the decrease of the total concentration. At a fixed total concentration, the change of composition has little effect on the pore size. (**a**) 8.76 wt% SF-2 wt% CS, (**b**) 3.72 wt% SF-2 wt% CS, (**c**) 2 wt% SF-2 wt% CS, (**d**) 1 wt% SF-2 wt% CS, (**e**) 2 wt% SF-1 wt% CS, (**f**) 1 wt% SF-3 wt% CS. Scale bar = 100 μm

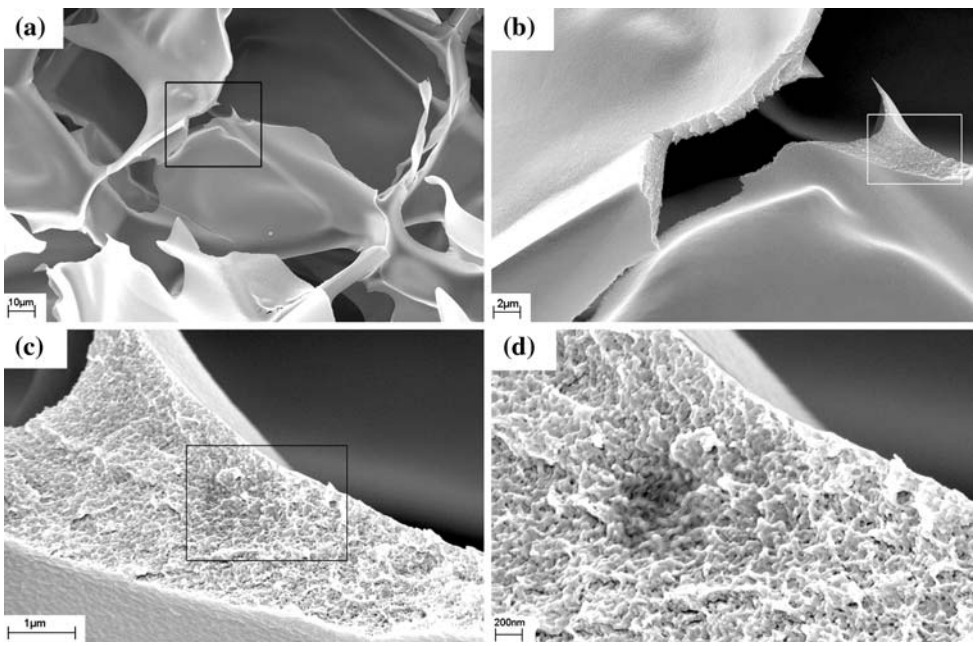

Fig. 2 SEM images of the pore wall surface and section morphology of 1 wt% SF-2 wt% CS SFCS scaffold. SF and CS are compatible very well even in nano-scale. Scale bar: (**a**) 10 μm, (**b**) 2 μm, (**c**) 1 μm, (**d**) 200 nm

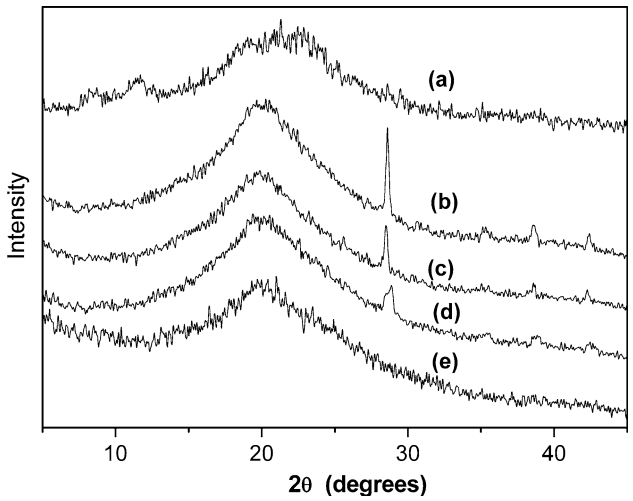

Fig. 3 X-ray diffraction curves of SFCS scaffolds and pure polymer scaffolds. Blending the two polymers has great effect on their original stuctures. (**a**) 4 wt% CS, (**b**) 1 wt% SF-3 wt% CS, (**c**) 2 wt% SF-2 wt% CS, (**d**) 3 wt% SF-1 wt% CS, (**e**) 3wt% SF

CS scaffold shows the peaks at 2θ 8.72, 11.7, and 22.88 respectively (Fig. 3a), corresponding to the crystal-structure of the anhydrous form of chitosan [31]. Pure SF scaffold shows the peaks at 2θ 8.5, 21, and 24.92 respectively (Fig. 3e), corresponding to the β-sheet crystalline structure (silk II) [32]. The weak peaks corresponding to the β-sheet crystalline structure indicate the low crystallinity of pure SF; thus pure SF exists mainly in random coil structure. SFCS scaffolds show the peaks at 2θ about 28.6, 38.6, and 42.4 (Fig. 3b–d), which do not exist in either pure SF or CS scaffolds. Furthermore, compared to pure SF or CS scaffolds, these peaks show much stronger intensities, especially for the peak at 2θ 28.6, and with the increase of SF content, their intensities decrease.

The FTIR spectra of pure SF, pure CS, and SFCS scaffolds are shown in Fig. 4. The pure CS scaffold shows peaks around 897 cm^{-1} and 1,154 cm^{-1} of assigned saccharide structure. It also shows the characteristic peaks of δ (N–H) resonance of CS at about 1,561 cm^{-1} [20]. The pure SF shows absorption bands at 1,653 cm^{-1} (amide I), 1,539 cm^{-1} (amide II), and 1,239 cm^{-1} (amide III), attributed to the SF with random coil conformation. When SF content in the blend scaffold is 25 wt%, the amide III of SF shows the peak at 1,257 cm^{-1}, which is attributed to the β-sheet conformation [33]. However, when SF content is 50 wt% and 75 wt%, the amide III of SF returns back to 1,242 cm^{-1} and 1,238 cm^{-1}, respectively, which is attributed to the random coil conformation. At the same time, the absorption band at 1,651 cm^{-1} for δ (N-H) resonance of CS disappeared, indicating the strong interaction between SF and CS.

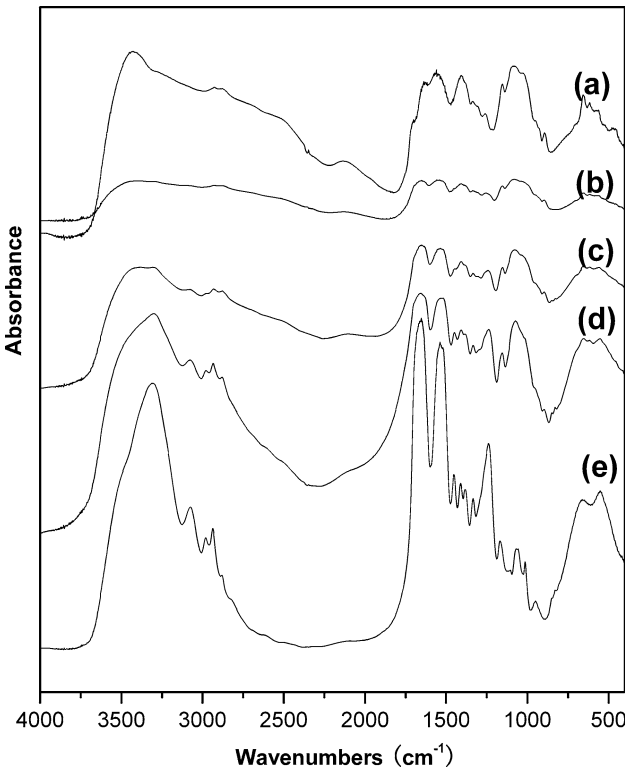

Fig. 4 FTIR spectra of SFCS scaffolds and pure polymer scaffolds: (**a**) 4 wt% CS, (**b**) 1 wt% SF-3 wt% CS, (**c**) 2 wt% SF-2 wt% CS, (**d**) 3 wt% SF-1 wt% CS, (**e**) 7.54 wt% SF

3.3 Mechanical properties

The compressive modulus and compressive strength for SFCS scaffolds are calculated according to stress-strain curves. When CS concentration is kept at a constant, 2 wt% (Fig. 5a, b), or 3 wt% (Fig. 5c, d), while increasing SF concentration, both compressive modulus and compressive strength for SFCS scaffolds increase ($P < 0.05$). In Fig. 5a and b, CS concentration is kept at 2 wt%. When SF concentration is 1 wt%, 2 wt%, and 3.72 wt%, the compressive modulus is 3.74, 5.08, and 12.17 MPa, and the compressive strength is 0.15, 0.25, and 0.61 MPa respectively. In Fig. 5c and d, CS concentration is kept at 3 wt%. When SF concentration is 0, 1 wt%, and 1.86 wt%, the compressive modulus is 3.07, 6.53, and 8.78 MPa, and the compressive strength is 0.11, 0.27, and 0.40 MPa respectively. From Fig. 5, we can also find out that when the SF concentration is kept at 1 wt%, with the increase of the CS concentration from 2 wt% to 3 wt%, the compressive modulus for SFCS scaffolds increases from 3.74 MPa to 6.53 MPa, while the compressive strength increases from 0.15 MPa to 0.27 MPa. These results demonstrate that we can increase the concentration of either SF or CS in SFCS scaffolds to get better mechanical properties.

Figure 6 shows how the change of silk fibroin content affects the mechanical properties of SFCS scaffolds

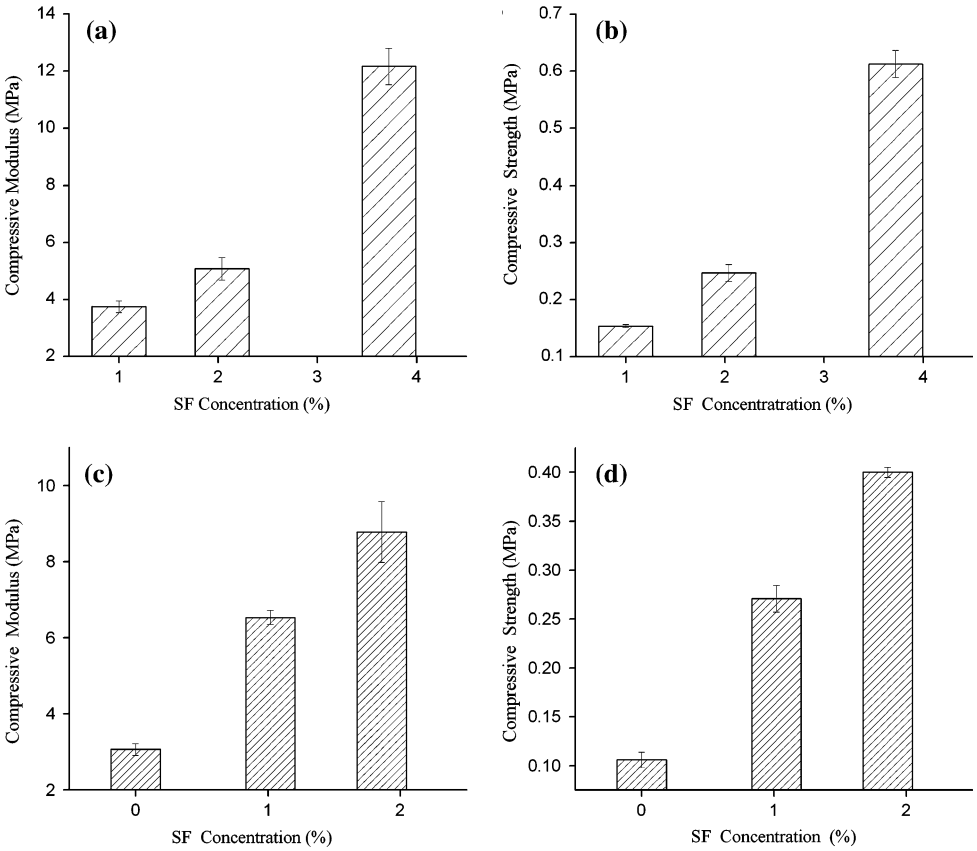

Fig. 5 Compressive modulus and compressive strength for SFCS scaffolds: (**a**), (**b**) CS concentration was kept at 2 wt%; (**c**), (**d**) CS concentration was kept at 3 wt%

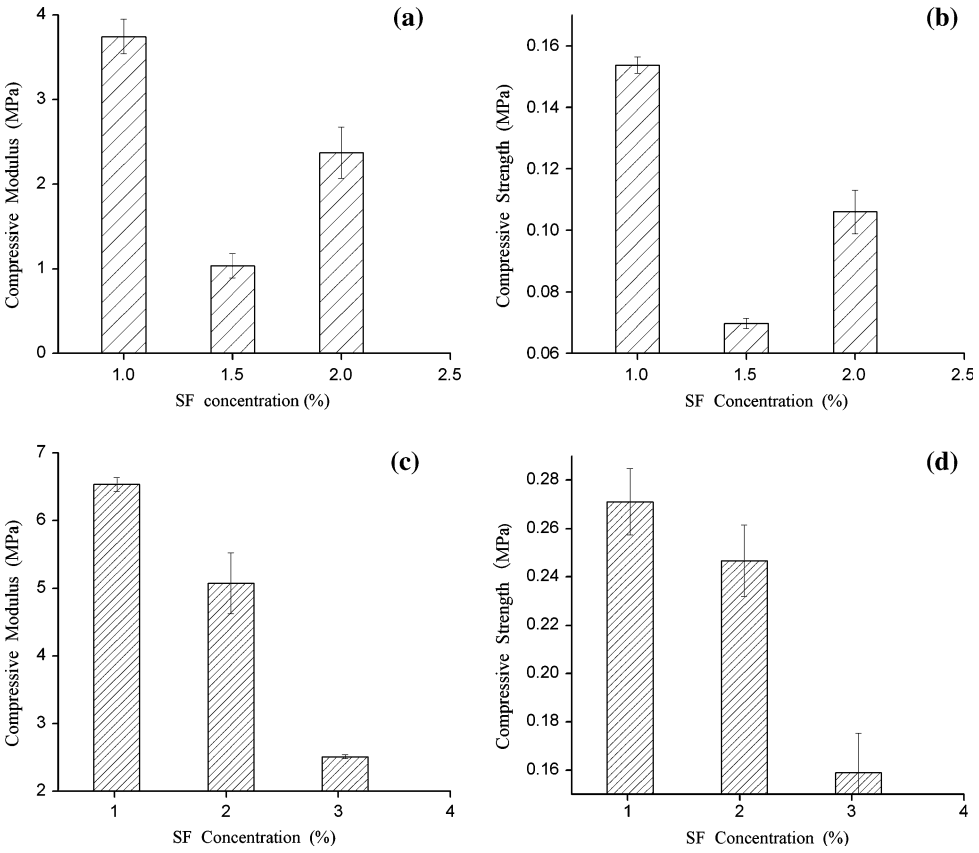

Fig. 6 Compressive modulus and compressive strength for SFCS scaffolds: (**a**), (**b**) the total concentration was kept at 3 wt%; (**c**), (**d**) the total concentration was kept at 4 wt%

Table 1 Porosity (%) of different SFCS scaffolds

Porosity (%)		Silk fibroin concentration (wt %)		
		3.72	2	1.5
Chitosan concentration (wt %)	2	95.43 ± 0.2	96.5 ± 0.1	–
	1.5	–	–	97.77 ± 0.4

Values are average ± standard derivation ($N = 3$). $P < 0.05$

when the total concentration of SF and CS is kept at a constant, 3 wt% (Fig. 6a, b), or 4 wt% (Fig. 6c, d). In Fig. 6c and d, the total concentration is kept at 4 wt%. Both the compressive modulus and compressive strength for the scaffold decrease with the increase of SF concentration ($P < 0.05$). But in Fig. 6a and b, when the total concentration is kept at 3 wt%, different phenomena appeared. The scaffold with 1.5 wt% SF has both the lowest compressive modulus and compressive strength. Increasing or decreasing the SF concentration increased the mechanical properties of the SFCS scaffold ($P < 0.05$).

3.4 Porosity

Table 1 shows the porosity of different SFCS scaffolds. All porosity values are above 95%. Porosity for SFCS scaffold increases, though not significantly, with the decrease of total concentration or SF concentration ($P < 0.05$). The porosity reaches 95.43% even though the total concentration becomes 5.72 wt%.

3.5 HepG2 cell culture

The proliferation of HepG2 cells on PLA scaffold and SFCS scaffold cultured for 3 and 5 days was compared by MTT assay. The data are shown in Fig. 7. Data of HepG2 cells cultured without scaffolds is also present. HepG2 cells proliferated well in both PLA and SFCS scaffolds, high above the HepG2 cells cultured without scaffolds, and there is no significant difference between PLA and SFCS.

4 Discussion

Three-dimensional SFCS scaffolds were successfully prepared. The morphology, structure and mechanical properties, as well as the HepG2 cell culture behavior of the SFCS scaffolds, were investigated.

The SFCS scaffolds are water-stable with controllable swelling properties, which is required in further in vivo study. SEM results (Fig. 1) demonstrate that we can mediate the porous structure by controlling the total, but not the SF concentration. At a certain total concentration,

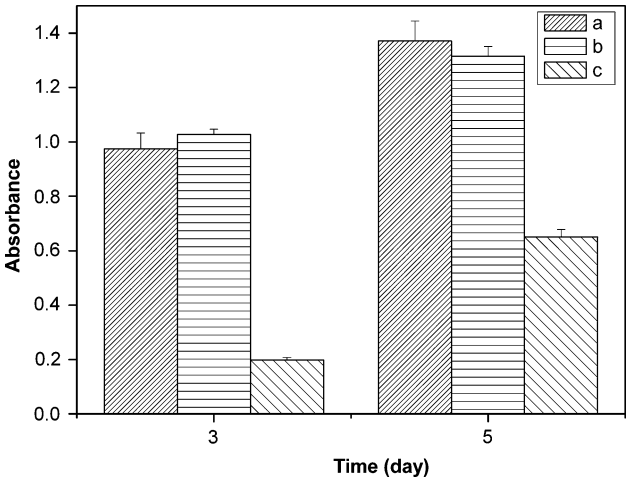

Fig. 7 MTT assay for the proliferation of HepG2 cell cultured in different scaffolds. The SFCS scaffold promote the proliferation of HepG2 cell greatly. (**a**) 4 wt% SF-1 wt% CS; (**b**) 6 wt% PLA; (**c**) without any scaffolds

we can change the SF content to meet the mechanical properties or other requirements without changing the morphology of the porous structure. The homogeneous pore wall section morphology (Fig. 2c, d) shows that SF and CS are compatible very well even in nano-scale. This result implies that SF and CS may be combined to generate a composite scaffold with both the advantages of these two natural derived biomaterials.

X-ray diffraction and FTIR spectra were employed to confirm the conformational changes of SFCS scaffolds. X-ray diffraction curves demonstrate that blending the two polymers has great effect on their original stuctures. Sung JP et al. [34] reported that crystallization of SF can be synergistically promoted by mixing 30 wt % CS with structural change from random coil form to β-sheet form. We do not get the result as they did, but we suppose that the structure change may be due to the strong hydrogen bonding between SF and CS. The FTIR spectra also demonstrate that blending of CS can induce the conformation change of SF, and strong molecular interaction exists between SF and CS. We suppose that it is the strong interaction between SF and CS that promotes the formation of homogeneous porous stucture, which is different from the sheet-like structure of SF.

Scaffolds should have proper strength and elastic modulus in order to retain their original shapes and to keep enough pore space. The mechanical results (Figs. 5, 6) demonstrate that the mechanical properties can be controlled by adjusting either the total concentration or the composition of SFCS scaffolds. Increasing the concentration of either SF or CS in SFCS scaffolds will get better mechanical properties. When the total concentration is kept at a constant, i.e. 4wt%, both the compressive modulus and

compressive strength for the scaffold decrease with the increase of SF concentration. Gobin et al. [13] have studied the mechanical properties of silk fibroin-chitosan blend scaffolds with the total concentration of 3.66 wt%. They reported that with the increase of SF content, the ultimate tensile strength and elastic modulus increased significantly. Though we measured the compressive modulus and strength, not the tensile strength and modulus as they did, these different results may be explained by the different structure of SFCS scaffolds we got. All scaffolds they got have sheet-like structure, most likely due to the β-sheet region of SF. Increasing the SF content may increase the β-sheet region, thus increase the strength and modulus. But scaffolds we got have homogeneous porous structure, most likely due to the good compatibility of SF and CS, which may cause new structure formation, as proved by X-Ray spectra. When total concentration was 4 wt%, increasing the SF concentration would affect the newly formed structure, thus decrease the mechanical properties. When total concentration was 3 wt%, the lowest compressive modulus and strength appeared at the intermediate level of SF concentration. We conjectured that the total concentration was as low as the critical concentration to fabricate the scaffolds, thus inducing this abnormal phenomenon.

Scaffolds for tissue engineering must have sufficient porosity for nutrient and gas exchange [6]. The porosities of SFCS scaffolds we prepared are all above 95%. The high porosity combined with interconnected porous structure make SFCS scaffolds suitable for tissue engineering.

Because both PLA and SFCS scaffolds have highly porous structure, they can provide much more surface and inner area for HepG2 cells to proliferate, compared to HepG2 cells cultured without scaffolds (Fig. 7). These results demonstrated that SFCS scaffolds have similar excellent cytocompatibility as PLA scaffold for the proliferation of HepG2 cells, and HepG2 cells can grow easily into the pores of SFCS scaffolds. So SFCS is not cytotoxic.

Both silk fibroin and chitosan have been widely studied because of their outstanding biological properties. Many researchers expected to combine these two natural polymers in order to get composite scaffold with better physical and biological properties [10, 13, 34–37]. But satisfactory three-dimensional scaffold has not been successfully fabricated until now.

The goal of our study is to develop a suitable scaffold for liver tissue engineering, and the SFCS scaffold may be a good choice. Dueing to its excellent physicochemical properties, the SFCS scaffold may be applied in other tissue engineering fields, such as nerve and cartilage tissue engineering etc.

In conclusion, blending of silk fibroin and chitosan into three-dimensional SFCS scaffold has been proved to be an effective way to provide a matrix with homogeneous porous structure, controllable pore size and mechanical properties. This matrix is also not cytotoxic. With the potential to load growth factors for tissue regeneration, SFCS scaffolds warrant further investigation in the field of tissue engineering. Further cell culture and animal experiment will be carried out to investigate the biocompatibility of this SFCS scaffold.

Acknowledgments This work is supported by National Basic Research Program of China (No. 2005CB623905) and the Foundation of Analysis and Testing in Tsinghua University.

References

1. C. Chan, F. Berthiaume, B.D. Nath, A.W. Tilles, M. Toner, M.L. Yarmush, Hepatic tissue engineering for adjunct and temporary liver support: Critical technologies. Liver Transpl. **10**, 1331–1342 (2004). doi:10.1002/lt.20229
2. L.E. Freed, G. Vunjaknovakovic, R.J. Biron, D.B. Eagles, D.C. Lesnoy, S.K. Barlow et al., Biodegradable polymer scaffolds for tissue engineering. Bio-Technology **12**, 689–693 (1994)
3. J. Mayer, E. Karamuk, T. Akaike, E. Wintermantel, Matrices for tissue engineering-scaffold structure for a bioartificial liver support system. J. Control. Release **64**, 81–90 (2000). doi:10.1016/S0168-3659(99)00136-4
4. D.W. Hutmacher, Scaffolds in tissue engineering bone and cartilage. Biomaterials **21**, 2529–2543 (2000). doi:10.1016/S0142-9612(00)00121-6
5. M.H. Sheridan, L.D. Shea, M.C. Peters, D.J. Mooney, Bioadsorbable polymer scaffolds for tissue engineering capable of sustained growth factor delivery. J. Control. Release **64**, 91–102 (2000). doi:10.1016/S0168-3659(99)00138-8
6. K.M. Kulig, J.P. Vacanti, Hepatic tissue engineering. Transpl. Immunol. **12**, 303–310 (2004). doi:10.1016/j.trim.2003.12.005
7. E. Torok, J.M. Pollock, P.X. Ma, C. Vogel, M. Dandri, J. Petersen et al., Hepatic tissue engineering on 3-dimensional biodegradable polymers within a pulsatile flow bioreactor. Dig. Surg. **18**, 196–203 (2001). doi:10.1159/000050129
8. J.J. Ge, Y.F. Cui, Y. Yan, W.Y. Jiang, The effect of structure on pervaporation of chitosan membrane. J. Membr. Sci. **165**, 75–81 (2000). doi:10.1016/S0376-7388(99)00228-8
9. D.K. Kim, H.S. Kim, Structure and characteristic of chitosan Bombyx mori silk fibroin blend films. Polym-Korea **29**, 408–412 (2005)
10. X. Chen, W.J. Li, W. Zhong, C.J. Ge, H.F. Wang, T.Y. Yu, Studies on chitosan-fibroin blend membranes. 2. The pH and ion sensitivities of semi-IPN membranes. Chem. J. Chin. U **17**, 968–972 (1996)
11. Q.A. Lv, Q.L. Feng, K. Hu, F.Z. Cui, Three-dimensional fibroin/collagen scaffolds derived from aqueous solution and the use for HepG2 culture. Polymer (Guildf) **46**, 12662–12669 (2005). doi:10.1016/j.polymer.2005.10.137
12. X.H. Wang, Y.N. Yan, F. Lin, Z. Xiong, R.D. Wu, R.J. Zhang et al., Preparation and characterization of a collagen/chitosan/heparin matrix for an implantable bioartificial liver. J. Biomater. Sci. Polym. Ed. **16**, 1063–1080 (2005). doi:10.1163/156856205479855 4
13. A.S. Gobin, V.E. Froude, A.B. Mathur, Structural and mechanical characteristics of silk fibroin and chitosan blend scaffolds for tissue regeneration. J. Biomed. Mater. Res. A **74A**, 465–473 (2005). doi:10.1002/jbm.a.30382
14. G.H. Altman, F. Diaz, C. Jakuba, T. Calabro, R.L. Horan, J.S. Chen et al., Silk-based biomaterials. Biomaterials **24**, 401–416 (2003). doi:10.1016/S0142-9612(02)00353-8

15. Y. Gotoh, N. Minoura, T. Miyashita, Preparation and characterization of conjugates of silk fibroin and chitooligosaccharides. Colloid Polym. Sci. **280**, 562–568 (2002). doi:10.1007/s00396-002-0658-3
16. M. Santin, A. Motta, G. Freddi, M. Cannas, In vitro evaluation of the inflammatory potential of the silk fibroin. J. Biomed. Mater. Res. **46**, 382–389 (1999). doi:10.1002/(SICI)1097-4636(19990905)46:3<382::AID-JBM11>3.0.CO;2-R
17. C.Z. Zhou, F. Confalonieri, M. Jacquet, R. Perasso, Z.G. Li, J. Janin, Silk fibroin: structural implications of a remarkable amino acid sequence. Proteins-Structure Funct. Genet. **44**, 119–122 (2001). doi:10.1002/prot.1078
18. R. Rujiravanit, S. Kruaykitanon, A.M. Jamieson, S. Tokura, Preparation of crosslinked chitosan/silk fibroin blend films for drug delivery system. Macromol. Biosci. **3**, 604–611 (2003). doi:10.1002/mabi.200300027
19. C.H. Du, B.K. Zhu, J.Y. Chen, Y.Y. Xu, Metal ion permeation properties of silk fibroin/chitosan blend membranes. Polym. Int. **55**, 377–382 (2006). doi:10.1002/pi.1995
20. H. Kweon, M.K. Yoo, I.K. Park, T.H. Kim, H.C. Lee, H.S. Lee et al., A novel degradable polycaprolactone networks for tissue engineering. Biomaterials **24**, 801–808 (2003). doi:10.1016/S0142-9612(02)00370-8
21. M.N.V.R. Kumar, A review of chitin and chitosan applications. React. Funct. Polym. **46**, 1–27 (2000). doi:10.1016/S1381-5148(00)00038-9
22. A. Di Martino, M. Sittinger, M.V. Risbud, Chitosan: a versatile biopolymer for orthopaedic tissue-engineering. Biomaterials **26**, 5983–5990 (2005). doi:10.1016/j.biomaterials.2005.03.016
23. A. Subramanian, D. Vu, G.F. Larsen, H.Y. Lin, Preparation and evaluation of the electrospun chitosan/PEO fibers for potential applications in cartilage tissue engineering. J. Biomater. Sci. Polym. Ed. **16**, 861–873 (2005). doi:10.1163/1568562054255682
24. B. Krajewska, Application of chitin- and chitosan-based materials for enzyme immobilizations: a review. Enzyme Microb. Technol. **35**, 126–139 (2004). doi:10.1016/j.enzmictec.2003.12.013
25. J.K.F. Suh, H.W.T. Matthew, Application of chitosan-based polysaccharide biomaterials in cartilage tissue engineering: a review. Biomaterials **21**, 2589–2598 (2000). doi:10.1016/S0142-9612(00)00126-5
26. S.V. Madihally, H.W.T. Matthew, Porous chitosan scaffolds for tissue engineering. Biomaterials **20**, 1133–1142 (1999). doi:10.1016/S0142-9612(99)00011-3
27. P.J. VandeVord, H.W.T. Matthew, S.P. DeSilva, L. Mayton, B. Wu, P.H. Wooley, Evaluation of the biocompatibility of a chitosan scaffold in mice. J. Biomed. Mater. Res. **59**, 585–590 (2002). doi:10.1002/jbm.1270
28. Q. Lv, S.J. Zhang, K. Hu, Q.L. Feng, C.B. Cao, F.Z. Cui, Cytocompatibility and blood compatibility of multifunctional fibroin/collagen/heparin scaffolds. Biomaterials **28**, 2306–2313 (2007). doi:10.1016/j.biomaterials.2007.01.031
29. S. Woodward, R.J. Thomson, Micropropagation of the silk tassel bush, Garrya elliptica Dougl. Plant Cell Tissue Organ. Cult. **44**, 31–35 (1996). doi:10.1007/BF00045910
30. T. Mosmann, Rapid colorimetric assay for cellular growth and survival: application to proliferation and cytotoxicity assays. J. Immunol. Methods **65**, 55–63 (1983). doi:10.1016/0022-1759(83)90303-4
31. T. Yui, K. Imada, K. Okuyama, Y. Obata, K. Suzuki, K. Ogawa, Molecular and crystal-structure of the anhydrous form of Chitosan. Macromolecules **27**, 7601–7605 (1994). doi:10.1021/ma00104a014
32. A.K. Tetsuo Asakura, R. Tabeta, H. Saito, Conformational characterization of Bombyx mori silk fibroin in the solid state by high-frequency carbon-13 cross polarization-magic angle spinning NMR, x-ray diffraction, and infrared spectroscopy. Macromolecules **18**, 1841–1845 (1985)
33. S. Sampaio, P. Taddei, P. Monti, J. Buchert, G. Freddi, Enzymatic grafting of chitosan onto Bombyx mori silk fibroin: kinetic and IR vibrational studies. J. Biotechnol. **116**, 21–33 (2005). doi:10.1016/j.jbiotec.2004.10.003
34. S.J. Park, K.Y. Lee, W.S. Ha, S.Y. Park, Structural changes and their effect on mechanical properties of silk fibroin/chitosan blends. J. Appl. Polym. Sci. **74**, 2571–2575 (1999). doi:10.1002/(SICI)1097-4628(19991209)74:11<2571::AID-APP2>3.0.CO;2-A
35. T. Nakamura, A. Teramoto, A. Hachimori, K. Abe, Preparation of silk fibroin-chitosan membranes and the effects on macrophage. Sen-I Gakkaishi **55**, 369–375 (1999)
36. H. Kweon, H.C. Ha, I.C. Um, Y.H. Park, Physical properties of silk fibroin/chitosan blend films. J. Appl. Polym. Sci. **80**, 928–934 (2001)
37. G.D. Kang, K.H. Lee, C.S. Ki, J.H. Nahm, Y.H. Park, Silk fibroin/chitosan conjugate crosslinked by tyrosinase. Macromol. Res. **12**, 534–539 (2004)